Investigation of the effect of bending twisting coupling on the loads in wind turbines with superelement blade definition

To cite this article: M O Gözcü and A Kayran 2014 *J. Phys.: Conf. Ser.* **524** 012040

Investigation of the effect of bending twisting coupling on the loads in wind turbines with superelement blade definition

M.O. Gözcü[1,3] and A. Kayran[2]

[1]Scientific Project Expert, METU Center for Wind Energy, METUWind,
Middle East Technical University, 06800, Ankara, Turkey
E-mail: gozcu@metu.edu.tr
[2]Professor, METU Center for Wind Energy, METUWind,
Middle East Technical University, 06800, Ankara, Turkey

Abstract. Bending-twisting coupling in the composite blades is exploited for load alleviation in the whole turbine system. For the purpose of the study, inverse design of a reference blade is performed such that sectional beam properties of the 3D blade design approximately match the sectional beam properties of NREL's 5MW turbine blade. In order to appropriately account for the bending-twisting coupling effect, dynamic superelement of the blade is created and introduced into the multi-body dynamic model of the wind turbine system. Initially, a comparative study is conducted on the performance of wind turbines which have blades defined as superelements and geometrically nonlinear beams, and conclusions are inferred with regard to the appropriateness of the use of superelement blade definition in the transient analysis of the 5MW wind turbine system that is set up in the present study. Multi-body dynamic simulations of the wind turbine system are performed for the power production load case with the constant wind and the normal turbulence model as external wind loadings. For the internal loads, fatigue damage equivalent load is used as the metric to assess the effect of bending-twisting coupling on the load alleviation in the whole wind turbine system. Results show that in the overall, through the bending-twisting coupling induced with the use of off-axis plies in the main spar caps of the blade, damage equivalent loads associated with the critical load components can be reduced in the wind turbine system.

1.Introduction

In the wind turbine industry, as the requirements for improved stiffness, fatigue life and reliability increase, to achieve these goals appropriate measures must be taken such that loads incurred due to the flexing of the blades must be alleviated. Exploiting bending-twisting coupling in composite blades in passive load control is considered as an alternative to the active load control strategies [1]. Internal loads in the wind turbine system are dynamic in nature with the load cycles exceeding 10^8 in the life time of the turbine system. Therefore, especially for wind turbine systems which have power output in the megawatt range, reducing the fatigue loads is very crucial to keep the turbine system operational for longer periods. Fatigue damage equivalent load is a sign of the degradation of the elements of the sub-structures of the wind turbine system due to material fatigue incurred under cyclic loading, and reduction in the damage equivalent loads implies increased fatigue life of the structural elements.

Most of the previous studies performed on the subject deal with effect of bending-twisting coupling on the loads acting on the blades rather than on the whole turbine system [1-6]. Different from most of

[3] To whom any correspondence should be addressed.

the work in the literature, in the current study, in addition to the effect of bending twisting coupling on the external aerodynamic load, the effect of bending-twisting coupling, generated in the turbine blades on the internal loads, such as shear force and bending moment, in the critical sub-structures of the whole wind turbine system is also investigated. For the purpose of the study, inverse design of a reference blade is performed such that sectional beam properties of the 3D blade design approximately match the sectional beam properties of NREL's 5MW turbine blade [7]. In order to appropriately account for the bending-twisting coupling effect, dynamic superelement of the blade is created and introduced into the multi-body dynamic model of the wind turbine system that is generated in Samcef Wind Turbines (SWT) [8]. Before the study of the effect of bending-twisting coupling on the loads acting on the wind turbine, a comparative study is conducted on the performance of wind turbines that have blades defined as superelements and geometrically nonlinear beams in SWT, and conclusions are inferred with regard to the appropriateness of the use of superelement blade definition in the transient analysis of the 5MW wind turbine system that is set up in the present study. Multi-body dynamic simulations of the wind turbine system are performed for the power production load case with the constant wind, and the normal turbulence model as external wind loadings as specified in IEC 61400-1 [9]. For the external loads, average values of the aerodynamic forces on the blades, which are determined through the unsteady blade element momentum method, are used for the assessment of the effect of bending-twisting coupling on the external load reduction. For the internal loads, fatigue damage equivalent load is used as the metric to assess the effect of bending-twisting coupling on the load alleviation in the whole wind turbine system. Time history results of aeroelastic simulations are used to calculate damage equivalent loads at the selected monitor points in the wind turbine system, and conclusions are inferred with regard to the effectiveness of the off-axis spar cap plies in the blade structure on the internal load alleviation. Glass-fiber-reinforced-plastic (GFRP) and carbon-fiber-reinforced-plastic (CFRP) materials are used in off-axis configuration in the spar caps of the blade to generate the bending-twisting coupling. A preliminary study is also conducted on the sensitivity of the flapwise stiffness and the associated bending-twisting coupling on the damage equivalent loads at the critical connection points in the wind turbine system that has blades with full GFRP material. It is concluded that with the introduction of bending-twisting coupling, damage equivalent loads can be reduced in the critical connection points of the whole wind turbine system, and not just in the blades. Proper adjustment of the bending-twisting coupling and flapwise stiffness is also necessary to achieve load reduction in the overall wind turbine system.

2. Inverse design of the reference blade and generation of the superelement of the blade

For the multi-body simulation of the wind turbine system, blades are usually modeled as coupled beams or dynamic superelements that are then introduced into the multi-body model of the wind turbine system. In either beam or superelement modeling approach of the blade, a three dimensional reference blade is needed to construct the beam or the superelement models of the blade so that the effect of coupling stiffness, such as bending-twisting coupling, on the load alleviation in the wind turbine system can be studied. In the current study, NREL's 5 MW turbine is taken as the reference turbine, and inverse design of a three dimensional blade is performed such that sectional beam properties of the baseline 3D blade approximately match the sectional beam properties of NREL's 5 MW turbine blade [7]. In the design of the reference turbine blade, initially GFRP is used as the base material. Based on the definitions of the airfoil sections given for the blade of NREL's 5 MW turbine, blade geometry is created by adjusting the cross-sections of the blade in the chordwise direction so that shear webs contain the pitch axis which passes through the center of the circular root section. In locating the positions of the shear webs, attention is also given such that shear webs are as close as possible to the maximum thickness of the airfoil sections. Inverse design of the reference blade is performed by following the flowchart shown in Figure 1. Inverse design starts with the preliminary design of the pressure/suction side and leading/training edge spar caps which have only unidirectional composite material. Biaxial composite laminates are defined in the regions between the leading/trailing edge spar caps and shear web spar caps on the suction and pressure side of the blade.

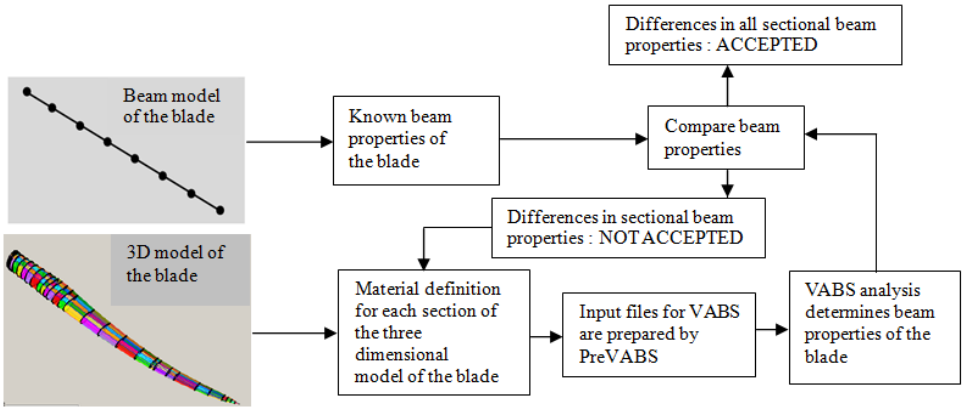

Figure 1. 3D design loop of a wind turbine blade with known sectional beam properties

For each section of the blade, appropriate laminate definitions are made for the suction and pressure side regions between the already designed spar caps. Two dimensional finite element models of blade sections are then prepared in PreVABS [10] whose output is processed by the variational asymptotic beam section code VABS [11] to calculate the sectional beam properties of the blade which are in turn compared with the known beam properties of the blade of NREL's 5 MW wind turbine system. Iterations continue until acceptable differences between the sectional beam properties are obtained for each section of the blade. The goal of the inverse design methodology is to come up with full GFRP blade design so that the design can be used as the baseline blade to study the effect of coupling stiffness on load alleviation. Figures 2 and 3 compare the sectional flapwise bending and torsional stiffness of the inverse designed blade and the NREL blade [7], respectively. It is seen that flapwise and torsional stiffness values of the inverse designed blade closely follow the trend of the corresponding stiffness properties of the NREL blade. For the edgewise bending stiffness, close agreement is also obtained between the inverse designed blade and the NREL blade.

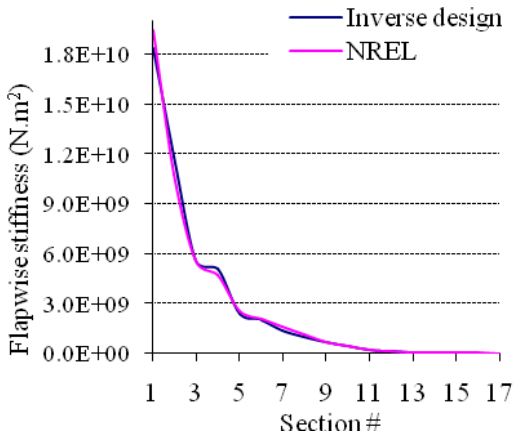

Figure 2. Flapwise bending stiffness of the inverse designed blade and the NREL blade

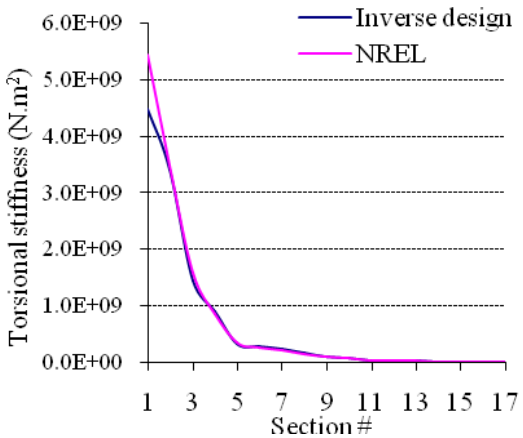

Figure 3. Torsional stiffness of the inverse designed blade and the NREL blade

It should be noted that although the final baseline blade may not be a production blade, baseline blade provides realistic stiffness and mass properties that nearly replicate the NREL's 5MW turbine blade. Following the initial inverse design of the blade, ply numbers are adjusted in some sections in order to obtain decreasing number of plies in the airfoil sections from blade root to the blade tip. Following the completion of the three dimensional design of the baseline blade with all the laminate

definitions across the blade span, dynamic superelement of the blade is generated in Samcef Field [12]. Dynamic superelement used in the present study is a nonlinear superelement that is based on the Craig and Bampton component mode method [13]. Nonlinearities arise from the fact that formulation of the superelement allows modeling of the blade structure undergoing large displacements and rotations in space associated with the rigid body rotation of the blade, with the only limitation that with respect to the local frame fixed to the blade, blade behaves geometrically linear. Dynamic superelement of the blade is then imported into the multi-body dynamic model of the complete wind turbine system that is created in SWT. The main advantage of using the dynamic superelement of the blade in the multi-body dynamic model of the wind turbine system is to allow the detailed modelling of components with complex geometry and structural function while keeping a relatively simple global dynamic model with the smallest number of degrees of freedom possible. It is noted that since dynamic superelement is created from three dimensional finite element model of the blade, superelement possesses the whole coupling effects. Verification of the superlement of the blade is done by performing modal analysis of the baseline blade which is clamped at the root. Free vibration frequencies of the first five modes obtained by the three dimensional finite element model of the blade are compared with the frequencies obtained by the modal analysis of the superelement of the blade in Table 1. First five modes include the major flapwise, edgewise bending and torsional modes of the blade. As it is seen from Table 1, good agreement exists between the natural frequencies obtained by the 3D finite element model and superlement of the blade. Such an agreement is an indication that the superelement of the blade represents the stiffness and the mass properties of the three dimensional blade accurately, and it can be included in the multi-body model of the complete wind turbine system with confidence.

Table 1. Comparison of first five frequencies of the turbine blade clamped at the root

Modes	3D FE Model (Hz)	Superelement Blade (Hz)
1	0.732	0.732
2	1.134	1.134
3	1.883	1.888
4	3.474	3.488
5	3.644	3.655

3.Comparative study of wind turbine simulation with superelement blades and geometrically nonlinear beam blades

To study the effect of bending twisting coupling on the load alleviation in the wind turbine system, a 5 MW multi-body wind turbine model is created in SWT. For realistic and reliable computation of the internal loads in the wind turbine system, several sub-structures, including the controller, must be present in the multi-body model of the turbine. For the parameters of the 5 MW wind turbine, known properties of NREL's 5 MW turbine is taken as the reference [7]. SWT integrates the aerodynamic, structural and control features of the wind turbine in a fully dynamic environment. Aerodynamic solver of SWT is based on BEM theory with typical corrections such as tip and hub losses, tower shadow and deactivation of induction factors at low tip speed ratios. SWT also has built-in semi-empirical sub-models to treat unsteady aerodynamics with higher accuracy. The controller is integrated to the wind turbine model by means of dynamic link library which can be used for typical wind turbine simulations. Multi-body simulation of the wind turbine system is performed by the implicit nonlinear finite element solver Samcef Mecano [14] which has the ability to allow the use of multi-body simulation features inside real finite elements models Transient simulations are performed in time domain taking into account the structural, multi-body, aerodynamic and control features in a fully nonlinear dynamic way with strong coupling. Figure 4 shows the wind turbine model created in SWT. Wind turbine model is composed of 61.5 m long blade with a 4 m prebent at the tip, an external

5MW controller, simple elastic beam model of tower that has a tower centerline elevation of 100 m, and standard models of bedplate, gearbox, rotor shaft, coupling shaft and the generator which are available in SWT. The standard gearbox selected has two planetary and one parallel gear stages with a gear box ratio of 105. Rotor has a 5^o tilt angle and together with the 4 m prebent at the tip, it is aimed to prevent possible blade tower collision during the operation of the wind turbine. Rated wind and rotational speeds of the wind turbine are 11.4 m/s and 12 rpm, respectively [7].

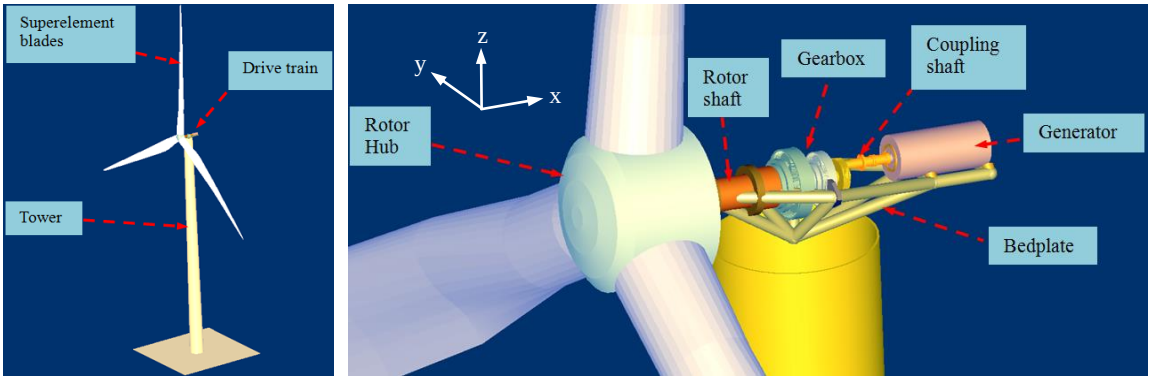

Figure 4. Multi-body dynamic model of the wind turbine system that is set up in SWT

Before the study of the effect of bending-twisting coupling on the loads acting on the wind turbine, a comparative study is conducted on the performance of the wind turbines which have blades defined as superelement and geometrically nonlinear beams in SWT. This study is performed in order to infer conclusions with regard to the appropriateness of the use of superelement blade definition in the transient analysis of the 5MW wind turbine system that is set up in the present study. For this purpose, two separate wind turbine models are generated in SWT. Except for the blades, both wind turbine models have the same sub-components shown in Fig.4. In both wind turbine models, blades are defined as bladed-rotor in SWT with pressure/suction side and leading/trailing edge spar caps having unidirectional GFRP layers all aligned with the blade axis. In this respect, blade configuration used in the comparative study has the lowest coupling stiffness. One of the wind turbine models is established by introducing the superelement of the blade, which is inverse designed, as the bladed-rotor definition in SWT. In the second wind turbine model, bladed-rotor is defined as geometrically nonlinear beam. The sectional beam properties of the beam blade are taken from the output of the variational asymptotic beam sectional analysis performed by VABS in the inverse design process of the reference blade. It should be noted that in SWT coupling stiffness are not included in the beam formulation. Therefore, blade defined as geometrically nonlinear beam only has major stiffness; flapwise, edgewise and torsional. On the other hand, superelement blade possesses the whole coupling effects with the only limitation that with respect to the local frame fixed to the blade, blade behaves geometrically linear. Multi-body simulation of the wind turbine is performed for constant wind speed that is taken as 15 m/s at the tower height with a wind shear factor of 0.2, and rated rotor speed is taken as 12 rpm. Multi-body simulations are performed for 240 seconds, and aerodynamic load is applied after 15 seconds of rotation of the turbine blades during which only the gravitational and centrifugal forces act on the blade. Fifteen seconds of rotation corresponds to three revolutions after which aerodynamic loading associated with the constant wind model is invoked. Figure 5 compares the peak axial displacements towards downwind (x direction in Fig. 4) at each section of blade calculated by the transient analysis of the wind turbine having superelement and geometrically nonlinear beam blade definitions. Peak displacements at each blade section are compared in the 20m-61.5m range. As expected, nonlinear beam blade has higher lower displacement towards downwind due to the geometric stiffening of the blade. Peak tip displacement of the superelement blade is 65 cm higher than the nonlinear beam blade. Table 2 gives the average and damage equivalent loads calculated at the at blade-hub link node of the superelement and nonlinear beam blade, respectively. Average and damage equivalent loads are calculated for the duration 25s-240s of the transient analysis and for the

damage equivalent load calculation fatigue exponent and reference number of cycles are taken as 4 and 10^8, respectively. Table 2 shows that average and damage equivalent loads calculated at the blade-hub link for the superelement and nonlinear beam blades are close to each other. The main differences are due to the nonlinear effects taken into account in the nonlinear beam blade, and coupling stiffness of the superelement blade which is mainly due to the blade geometry since the baseline blade has all spar plies aligned along the blade span. It should be noted that in the study of the effect of bending-twisting coupling on the load alleviation, percent difference of damage equivalent loads are used. Therefore, results of the preliminary analysis suggest that superelement blade can be used in the multi-body dynamic model of the wind turbine system for the study of the effect of bending-twisting coupling on the load alleviation in the wind turbine system.

Figure 5. Comparison of peak axial displacements towards downwind

Table 2. Comparison of average and damage equivalent loads at blade-hub link node

	Fx:Leadwise Force (N)	Fz:Spanwise Force (N)	Mx:Leadwise Moment (Nm)	My:Flapwise Moment (Nm)
Superelement blade				
Average loads	151,293	579,688	1,241,145	4,945,262
Damage Equivalent Loads	1,505	8,835	175,525	52,653
Nonlinear beam blade				
Average loads	146,363	535,043	1,243,720	5,034,572
Damage Equivalent Loads	2,004	8,377	162,217	73,518

4. Effect of GFRP/CFRP off axis spar cap plies on the load alleviation in the wind turbine system

Multi-body simulation of the wind turbine system with superelement blade definition is performed in Samcef Wind Turbines for the power production load case using the normal turbulence model as the external wind loading, as specified in IEC 61400-1. Wind speed at the reference height is taken as 15 m/s with a wind shear factor of 0.2, and for the normal turbulence wind condition, Kaimal turbulence model is used for the generation of the aerodynamic loading. For the turbulent wind load case, the duration of the transient analysis is taken as 615 seconds, but in accordance with IEC-61400-1, damage equivalent loads are calculated for the duration of 600 seconds, excluding the initial 15 seconds of rotation of the turbine which corresponds to 3 revolutions. In the turbulent wind analyses, IEC wind turbine class is taken as 1 and turbulence class is selected as B. Turbulent wind generator in Samcef Wind Turbine uses Turbsim stochastic inflow turbulence tool developed by NREL. In the present study, baseline blade has full GFRP material with 0^o fiber orientation in the spar caps. Zero degree orientation is defined as the axis which traverses the blade from blade root to the blade tip

through the middle of the spar caps. To induce bending-twisting coupling, GFRP and CFRP materials are used in off-axis configuration in the spar caps. Transient aeroelastic analysis of the complete wind turbine system is first performed for the turbine with baseline blades having 0^o spar cap plies, and then for the turbine with blades having 15^o off-axis spar cap plies. Figure 6 shows the inverse designed blade and the 18 sections where retained nodes are defined in the superelement blade. Retained nodes are defined at the aerodynamic center of each section, and these nodes are tied to the nodes in the left and right neighbouring surfaces by mean elements. For coupled blades, in order to exploit the bending-twisting coupling effect effectively, for both GFRP and CFRP cases, off-axis plies are placed in the main pressure and suction side spar caps in the 30 m of the blade measured from the blade tip.

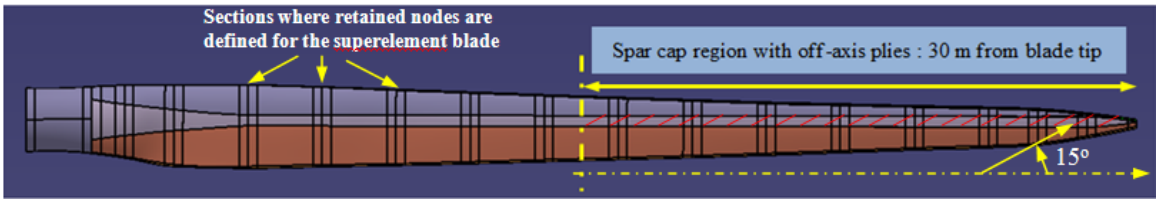

Figure 6. Inverse designed blade and spar cap region with off-axis plies

For the GFRP blade and 0^o and 15^o spar cap ply cases, Figure 7 shows the average sectional lift values, which are calculated for the transient analysis duration of 600s. It is noticed that in the outboard sections of the blade that has 15^o off-axis spar cap plies; there are reductions in the lift. In the inboard sections of the blade, lift increases due to the decrease in the pitch angle of the blade to produce the required torque for the 5 MW energy production. It should be noted that during the 600s of transient analysis, average pitch angle of the blade with 0^o spar cap ply is calculated as 8.19^o, whereas for the blade with 15^o spar cap ply average pitch angle is 7.73^o. The main reason for the increase in the lift in the inboard sections of the blade, that has 15^o spar cap plies in the outboard sections, is the difference in the pitch angles. However, with the introduction of off-axis spar cap plies in the outboard sections of the blade, reductions have been obtained in damage equivalent loads at the blade root and at other critical points in the wind turbine system. For the turbulent wind load case, Table 3 summarizes the damage equivalent moments calculated at the root of the blade for turbines having blades with GFRP and CFRP off axis spar cap plies. For the off-axis spar cap ply configurations, damage equivalent loads are calculated with respect to the reference blade which has 0^o GFRP spar cap plies that are oriented along the blade axis.

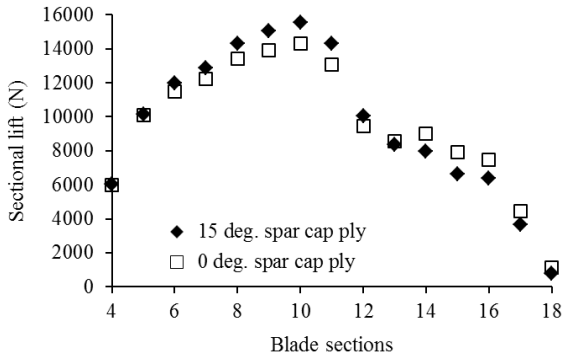

Figure 7. Comparison of lift in blades sections for the 0^o and 15^o spar cap ply cases

For the 15^o CFRP case, ply numbers are adjusted such that the differences between the flapwise and edgewise bending and torsional stiffness of the blades with 15^o GFRP and CFRP spar cap plies are minimized. From Table 3, it is seen that with the introduction of off-axis CFRP spar cap plies in the blades, higher reductions in the damage equivalent loads can be achieved. The higher reduction in the leadwise moment is attributed to the lower weight of the blade with CFRP off-axis spar cap plies. It

should be noted that for a rotating blade, the cyclic load associated with the weight of the blade mainly affects the leadwise moment. For the GFRP case, damage equivalent leadwise moment increases slightly due to the decrease in the flapwise stiffness and the associated increase in the bending-twisting coupling and slight decrease in the leadwise bending stiffness.

Table 3. Damage equivalent blade root moments calculated for the turbulent wind load case[a]

Damage equivalent (DE) blade root moments (Nm)	GFRP Spar Cap			CFRP Spar Cap	
	0^o spar cap	15^o spar cap	Ratio of DE moments ($15^o/0^o$ GFRP)	15^o spar cap	Ratio of DE moments ($15^o/0^o$ GFRP)
Leadwise moment	203448	204610	1.01	173039	0.85
Flapwise moment	132718	120617	0.91	116530	0.88
Torsional moment	3985	3993	~1	3576	0.9

[a]Mean wind speed: 15 m/s, Duration: 15-615 seconds, Fatigue exponent=4, Number of bins=240

Figure 8 shows the main shaft main bearing 1 and main shaft gearbox connection points. In the drive train model that is set up in SWT, main bearing 1 is the bearing which is closer to the rotor and it takes all the axial force in the main shaft, and main bearing 2 only takes the lateral forces. Forces and moments at the main bearing 1 and shaft-gearbox connection are calculated with respect to hub-fixed coordinate system located at the main bearing 1. Table 4 presents the damage equivalent loads calculated at the main bearing 1 and main shaft gearbox connection points for the turbulent wind load case. From Table 4, it is seen that for the wind turbine that has GFRP off-axis spar cap plies in the blades, % 4 - %10 reductions in damage equivalent forces in main bearing 1 can be achieved. The reduction in the axial damage equivalent x-force is highest, because x-force is related to the thrust force component of the lift force acting on the blades. For the CFRP spar cap case, the reduction in damage equivalent x-force at the main bearing 1 is even higher due to the higher reduction in the lift. Reduction in main bearing forces is very important in terms of decreasing the bearing failures associated with the fatigue loading in the long operation times of the wind turbine system.

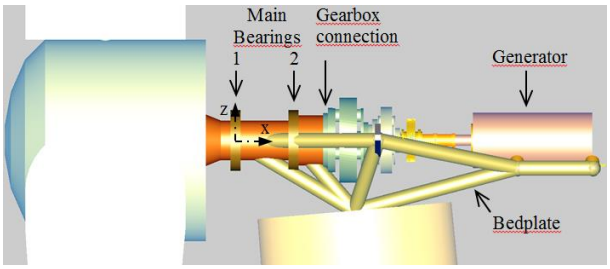

Figure 8. Main bearing 1 and shaft-gearbox connection

At the main shaft gearbox connection, damage equivalent x-force is not calculated since the axial force in the rotor system is taken by the main bearing 1. From Table 4, it is seen that for both GFRP and CFRP off-axis spar cap ply cases, similar to the reduction in damage equivalent main bearing 1 y and z forces, damage equivalent y and z forces at the main shaft gearbox connection point also drop compared to the wind turbine system with the baseline blade with 0^o spar cap plies. It should be noted that y and z forces correspond to the shear forces at the bearing or at the shaft-gearbox connection locations. At the shaft-gearbox connection, reduction is also observed in the damage equivalent y and z bending moments. However, damage equivalent x-moment increases for both GFRP and CFRP off-axis ply cases. It is noted that gear box connection x-moment at the hub-blade connection point is essentially the useful aerodynamic torque that flows into the gearbox. The torque entering the gearbox is transmitted to the generator through the gearbox via the tangential forces in the planetary and parallel gear stages.

Table 4. Damage equivalent loads calculated at main shaft/bedplate/gearbox connections

Locations	Damage equivalent loads (N - Nm)	GFRP Spar Cap			CFRP Spar Cap	
		0^o spar cap	15^o spar cap	Ratio of DE loads ($15^o/0^o$ GFRP)	15^o spar cap	Ratio of DE loads ($15^o/0^o$ GFRP)
Main Bearing 1	x-force	5866	5251	0.90	4929	0.84
	y-force	88414.5	83189	0.94	82499	0.93
	z-force	79560	76325	0.96	76526.5	0.96
Gearbox Connection	y-force	9492	9002	0.95	8992	0.95
	z-force	9316	9007	0.97	9089	0.98
	x-moment	5515	5770	1.05	6624	1.2
	y-moment	7615	7403	0.97	7466	0.98
	z-moment	7608	7179	0.94	7139	0.94

To investigate possible ways of reducing the damage equivalent torque entering into the gearbox, a study is conducted on the sensitivity of the flapwise stiffness and the associated bending-twisting coupling and the leadwise bending stiffness on the damage equivalent loads for blades with GFRP spar caps without increasing the weights of the blades. For this purpose, two new blades are designed. In the first blade, certain number of 15^o spar cap plies are converted into 0^o such that flapwise stiffness of the blade sections in the outboard 30 m of the blade increased approximately by %10, and bending-twisting coupling stiffness coefficients decreased in the range of %25-%38. In the second blade, 15^o to 0^o conversion is made such that flapwise stiffness of the blade sections in the outboard 30 m of the blade increased approximately by %15, and bending-twisting coupling stiffness coefficients decreased by %38-%50. In both cases, leadwise stiffness of the blades slightly increase due to the increase of flapwise stiffness. Table 5 gives the comparison of the ratio of the damage equivalent loads in the wind turbine with blades having 15^o spar cap plies to the damage equivalent loads in the turbine with the baseline blade. With the modifications in the outboard sections of the blade, it has been possible to reduce the damage equivalent torque entering into the gearbox at the cost of lower reductions in the damage equivalent loads at other connection points in the wind turbine system. Preliminary study showed that with careful adjustment of the blade stiffness, reductions in damage equivalent loads in the connection points of the whole wind turbine system, not just in the blades, can be possible.

Table 5. Comparison of the ratio of damage equivalent loads of GFRP blades with 15^o spar cap ply

Ratio of DE loads for turbine with GFRP blades (blade with 15^o spar cap/blade with 0^o spar cap)			
Damage Equivalent Loads	Original blade with 15^o spar cap	Flapwise stiffness is increased by %10	Flapwise stiffness is increased by %15
Blade root leadwise moment	1.01	1.00	1.00
Blade root flapwise moment	0.91	0.94	0.96
Blade root torsional moment	~1	1.00	1.00
Main bearing 1 x-force	0.90	0.92	0.94
Main bearing 1 y-force	0.94	0.96	0.97
Main bearing 1 z-force	0.96	0.98	0.99
Gearbox connection y-force	0.95	0.96	0.98
Gearbox connection y-force	0.97	0.98	0.99
Gearbox connection x-moment	1.05	1.02	1.01
Gearbox connection y-moment	0.97	0.98	0.99
Gearbox connection z-moment	0.94	0.96	0.98

5. Conclusion

The effect of bending-twisting coupling, induced via off-axis spar cap plies in the blade, on the loads in a wind turbine system with superelement blade definition is investigated. Based on the results of the multi-body simulations of the wind turbine system with superelement blade and non-linear beam blade, it is concluded that superelement blade may be used in the multi-body dynamic model of the

wind turbine system for the study of the effect of bending-twisting coupling on the load alleviation. With the use of off-axis CFRP spar cap plies in the blades, higher reductions in the damage equivalent loads can be achieved compared to GFRP spar cap ply case. It is concluded that with the introduction of bending-twisting coupling, damage equivalent loads can be reduced in the critical connection points of the whole wind turbine system, and not just in the blades. Preliminary study conducted on the sensitivity of the flapwise stiffness and the associated bending-twisting coupling on the damage equivalent loads for blades with GFRP spar cap plies showed that damage equivalent torque entering into the gearbox could be reduced, compared to the original off-axis blade configuration, at the cost of lower reductions in the damage equivalent loads at other connection points in the wind turbine system. It is considered that by using hybrid GFRP/CFRP plies in the spar caps, and adjusting the sectional stiffness accordingly, higher reductions in damage equivalent loads in the critical connection points of the whole wind turbine system can be achieved. To further substantiate the outcome of the present study, load reduction study must be coupled with the blade design process and comprehensive study of the effect of blade stiffness on the damage equivalent loads must be performed. For maximum load reduction, controllers that are actually optimized for wind turbine systems that have bend-twist coupled blades must be developed rather than the standard controller that is used in the present study.

Acknowledgments
This work was supported by the Metu Center for Wind Energy and Scientific and Technological Research Council of Turkey (TÜBİTAK), Project No: 213M611.

References

[1] Locke J, Valencia U 2004 *Design Studies for Twist-Coupled Wind Turbine Blades* Sandia National Laboratories Report No. SAND2004-0522
[2] Kooijman H J T 1996 *Bending-Torsion Coupling of a Wind Turbine Rotor Blade* ECN-I-96-060 Report
[3] Luczak M, Manzato S, Peeters B, Branner K, Berring P and Kahsin M 2011 *Dynamic Investigation of Twist-Bend Coupling in a Wind Turbine Blade* Journal of Theoretical and Applied Mechanics **49 (3)** 765
[4] Lin H J, Lai W M 2010 *A Study of Elastic Coupling to the Wind Turbine Blade by Combined Analytical and Finite Element Beam Model* Journal of Composite Materials **44** 2643
[5] Capellaro M 2012 *Design Limits of Bend Twist Coupled Wind Turbine Blades* 53rd AIAA/ASME/ASCE/AHS/ASC Structures Structural Dynamics and Materials Conference AIAA 2012-1501 Honolulu Hawaii USA
[6] EU UpWind Project, UpWind 2011 *Design limits of solutions for very large wind turbines* 6th Framewok Programme
[7] Jonkman , Butterfield S, Musial W and Scott G 2009 *Definition of a 5-MW Reference Wind Turbine Offshore System Development* National Renewable Energy Laboratory NREL/TP 500-38060
[8] Samcef Wind Turbines (SWT), http://www.lmsintl.com/simulation/wind-turbines last accessed date: 16/12/2013
[9] International Standard, IEC 61400-1 2005 *Wind Turbines – Part 1: Design Requirements* Third edition 2005-08 International Electrotechnical Commission Switzerland
[10] Chen H and Yu W 2008 *Manual of PreVABS* December http://analyswift.com/wp-content/uploads/2012/10/PreVABS-Manual.pdf last accessed date: 30.03.2014
[11] Yu W 2011 *VABS Manual for Users* http://analyswift.com/wp-content/uploads/2012/10/VABS-Manual.pdf last accessed date: 05.05.2013
[12] Samcef Field, http://www.lmsintl.com/samcef-field, last accessed date: 30.03.2014
[13] Kammer D C, Baker M 1986 *Comparison of the Craig-Bampton and Residual Flexibility Methods of Substructure Representation* Journal of Aircraft **24(4)** 262
[14] Samcef Mecano http://www.lmsintl.com/?sitenavid=8435E5BB-C04D-49AB-B72A-9CB01D6FD9DB last accessed date: 30.03.2014